Study of the EFG Trends in Zr_2T (T = Fe, Co, Ni) Intermetallic Compounds *

H. M. Petrilli [a], M. Marszalek [b], and H. Saitovitch [c]

[a] Instituto de Física da USP, Cx. P. 66318, 05389-970, São Paulo, SP, Brazil
[b] H. Niewodniczanski Institute of Nuclear Physics, Radzikowskiego 152, 31-342 Cracow, Poland
[c] Centro Brasileiro de Pesquisas Físicas, Rio de Janeiro, Brazil

Z. Naturforsch. **51a**, 537–543 (1996); received February 13, 1996

We use the linear muffin-tin orbital formalism, in the atomic sphere approximation, to investigate the trends of the electric field gradient (EFG) at the nucleus for the non-equivalent sites in Zr_2T (T = Fe, Co and Ni) intermetallic compounds. As all those compounds crystallize in the same C16 crystallographic structure, they offer a rare opportunity to investigate electronic structure effects coming from transition metals on the EFG at Zr site. Those results are compared with EFG values obtained from quadrupole coupling constant measurements performed with the time differential perturbed angular correlation (TDPAC) technique, using the ^{181}Ta probe.

Key words: Electric Field Gradient; Intermetallic Compounds; LMTO-ASA; Electronic Structure; Nuclear Quadrupole Interactions.

Introduction

In this paper we present first-principles local spin density calculations for the (dominant) electronic contribution to the EFG in Zr_2T (T = Fe, Co, Ni) intermetallic compounds. As all those compounds have the same crystalline structure of C16 type, they are specially suited to investigate electronic structure effects on the EFG at the Zr site, when the transition metal T is varied. For the theoretical electronic structure calculations we use the well known self consistent *"Linear Muffin-Tin Orbital in the Atomic-Sphere Approximation"* [1] (LMTO-ASA) method in a scalar relativistic version. From the LMTO-ASA charge density we calculate the EFG tensor, whereby no empirical factors are used. This procedure to evaluate the EFG may be found in the literature as a successful approach used in different self consistent band structure methods [2–8].

In the present study, the EFG's calculated at the Zr sites in Zr_2T compounds are compared with time differential perturbed angular correlation (TDPAC) measurements performed at a ^{181}Ta probe impurity [9, 10]. With the TDPAC technique the electric quadrupole interaction between the nuclear quadrupole moments of radioactive probe atoms and extranuclear EFGs can be measured. The structure of the studied compounds [11] is C16 base centred tetragonal with only one crystallographic position of the Zr atom. Accordingly only one EFG was observed [9, 10], and its absolute value increased at the Zr site when going through the 3d metal series from Ni to Fe. As will be shown, these trends are confirmed by theoretical calculations, where also the EFG sign is available. A direct comparison of experimental and theoretical EFG values is not possible because of the presence of the ^{181}Ta probe at the Zr site in the measurements. Therefore, we have also investigated the impurity probe effects upon the EFG. This information may help experimentalists in the interpretation of other data. For completeness we also calculated the EFG at the T site, although not all the experimental values are available in the literature.

1. Theoretical Approach

The LMTO-ASA formalism is well known [1, 12]. A detailed description of the theoretical procedure used here can be found in [4, 7, 8].

In this paper we use the standard *k*-space LMTO-ASA (without the so called combined corrections) to obtain the electronic structure and the EFGs for the Zr_2Fe, Zr_2Co and Zr_2Ni intermetallic compounds. Scalar relativistic calculations were performed, yield-

* Presented at the XIIIth International Symposium on Nuclear Quadrupole Interactions, Providence, Rhode Island, USA, July 23–28, 1995.

Reprint requests to Dr. H. M. Petrilli.

0932-0784 / 96 / 0500-0537 $ 06.00 © – Verlag der Zeitschrift für Naturforschung, D-72072 Tübingen

ing the corresponding charge density inside each wigner-seitz (WS) sphere. By solving Poisson's equation for the total (electronic plus nuclear plus core) charge density, the electrostatic potential is calculated. The leading terms of the $l = 2$ components of this potential near the nucleus determine the EFG tensor components $\bar{V}_{ij}$ $(i, j = x, y, z)$ in a system of axes parallel to the crystal (a, b and c)-axes. The diagonalization of this 3 by 3 matrix gives the EFG components in the local principal axes. The measured EFG is associated with the component of the diagonal tensor with the largest absolute value defined as V_{zz}. This diagonalization, corresponding to a rotation of the original axes, enables also to determine the eigenvectors of these rotation axes (that is the direction cosines of the EFG components), so we can also determine the direction of the EFG. Another measurable quantity that can be obtained from the components of the diagonal EFG tensor is the asymmetry parameter η, given by

$$\eta = \left| \frac{V_{xx} - V_{yy}}{V_{zz}} \right| . \tag{1}$$

We note that we are using throughout this paper the following notation: $\bar{V}_{ij}$ for the EFG tensor components expressed in the original system of axes, that are parallel to the a, b and c axes; V_{ij} (without upper bar) for the EFG tensor components expressed in the local principal axes (where the tensor is diagonal). As it has been pointed out before [3, 4, 6–8, 13], the EFG can conveniently be analysed as a product of two different contributions which are combined to give the p and d contributions: one radial integral (I_{pp} or I_{dd}) and an angular asymmetry (Δn_p or Δn_d). The angular asymmetries are mainly given by the difference in occupations of orbitals with different m quantum number (different symmetries) and are responsible for the EFG sign. The radial integrals are usually the main responsible ones for the order of magnitude of a given p or d contribution.

2. Results and Discussion

We have applied the scalar-relativistic LMTO-ASA method to calculate the electronic structure for the three crystalline alloys Zr_2T (T = Fe, Co, Ni) and the EFG at each nonequivalent site. The three crystalline compounds considered here crystallize in the $CuAl_2$ (C16)-type structure (space group I4/mcm, D_{4h}^{18}). The (001) projection of the ideal AB_2 C16-type structure is given in Figure 1. The full crystallographic data of those compounds can be found in [11]. The Zr atoms in this structure form two sets of mutual orthogonal planes with a dense packing of hexagons. These hexagons are regular if $c/a = (2/3)^{1/2} \cong 0.817$ and $x = (1/6) \cong 0.167$, values that are very close to the c/a and x values observed in Zr_2Ni. We also note that Zr_2Co and Zr_2Fe present very similar crystallographic parameters. Due to the crystallographic structure, only one T site and one Zr site have to be considered in the calculations. The presently obtained total local density of states (LDOS) and its partial s, p and d contributions for the T and Zr site are shown in Figure 2. The total LDOS are shown in Figure 3. The WS radius (R_{ws}^{T} and R_{ws}^{Zr}) used in the calculations, the obtained sphere charges (QSPH) and density of states at the Fermi level $N(E_f)$ per primitive cell, are shown in Table 1. The WS radius was chosen in order to take account of the metallic atomic size and, as a

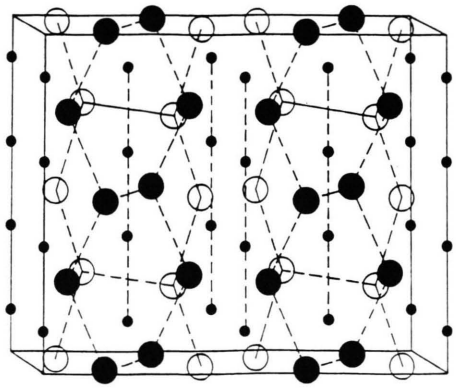

Fig. 1. The (001) projection of the C16-type structure. The Zr atoms lying in the (110) plane are dark to distinguish them from Zr atoms in the (1$\bar{1}$0) plane. The T (T = Fe, Co or Ni) atoms have smaller diameters than the Zr atoms.

Table 1. Wigner-Seitz radius R_{ws}^{T} and R_{ws}^{Zr} in Å and corresponding sphere valence electronic charges $QSPHT^{T}$ and $QSPH^{Zr}$ of the T and Zr sites in the Zr_2T (T = Fe, Co, Ni) compounds. $N(E_f)$ is the density of states in states per Ry per primitive cell.

Zr_2T	Zr_2Fe	Zr_2Co	Zr_2Ni
R_{ws}^{Zr}	1.759	1.753	1.749
$QSPH^{Zr}$	4.072	4.052	4.035
R_{ws}^{T}	1.362	1.372	1.400
$QSPH^{T}$	9.912	8.914	7.927
$N(E_f)$ (Total/cell)	86.6	99.9	106.4

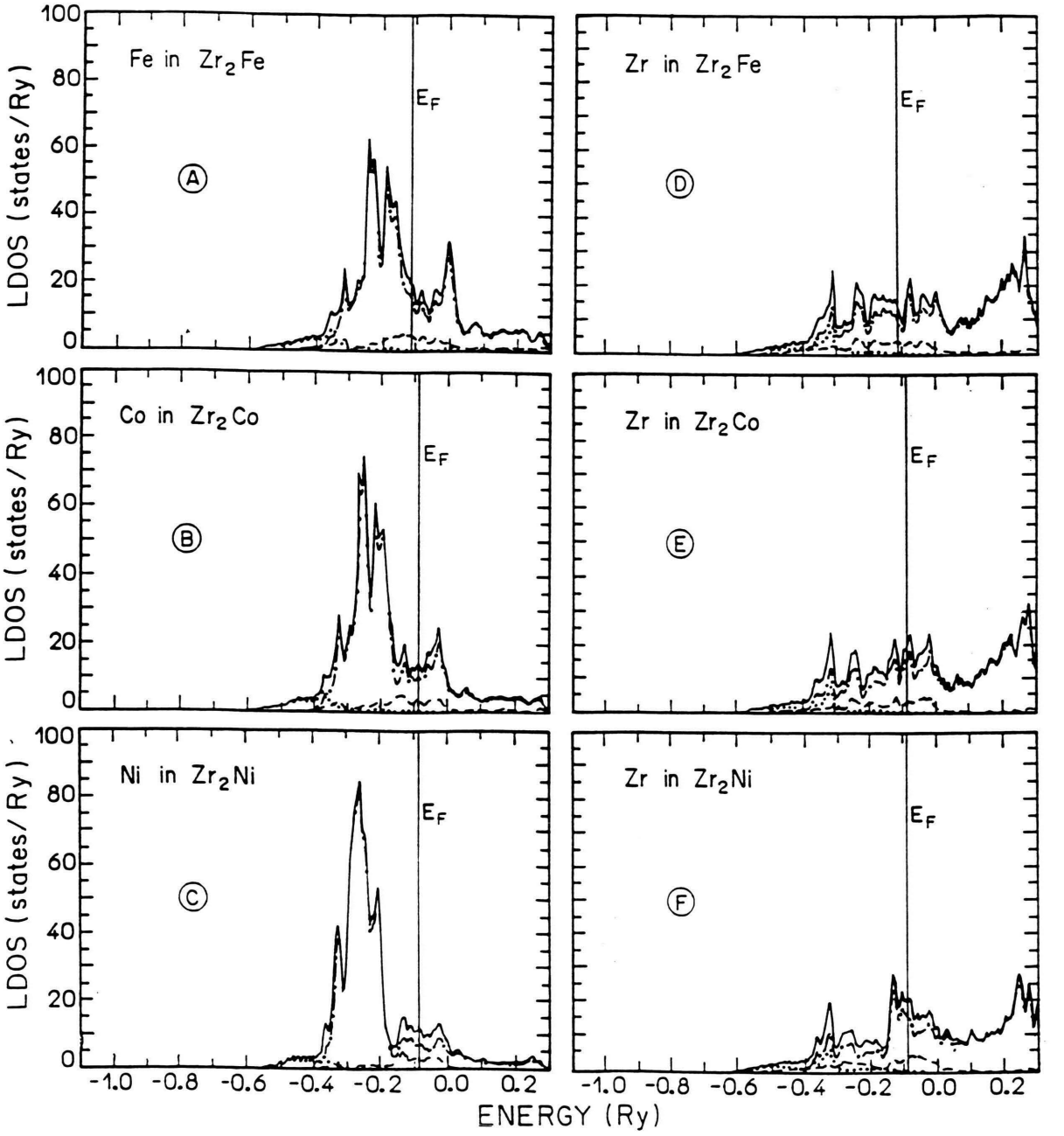

Fig. 2. Total local density of states per atom (solid line) and its projected *s* (·····), *p* (– – – –) and *d* (–·–·–) contributions at Zr and T sites in Zr_2T compounds: (A) Fe in Zr_2Fe; (B) Co in Zr_2Co; (C) Ni in Zr_2Ni; (D) Zr in Zr_2Fe; (E) Zr in Zr_2Co; (F) Zr in Zr_2Ni.

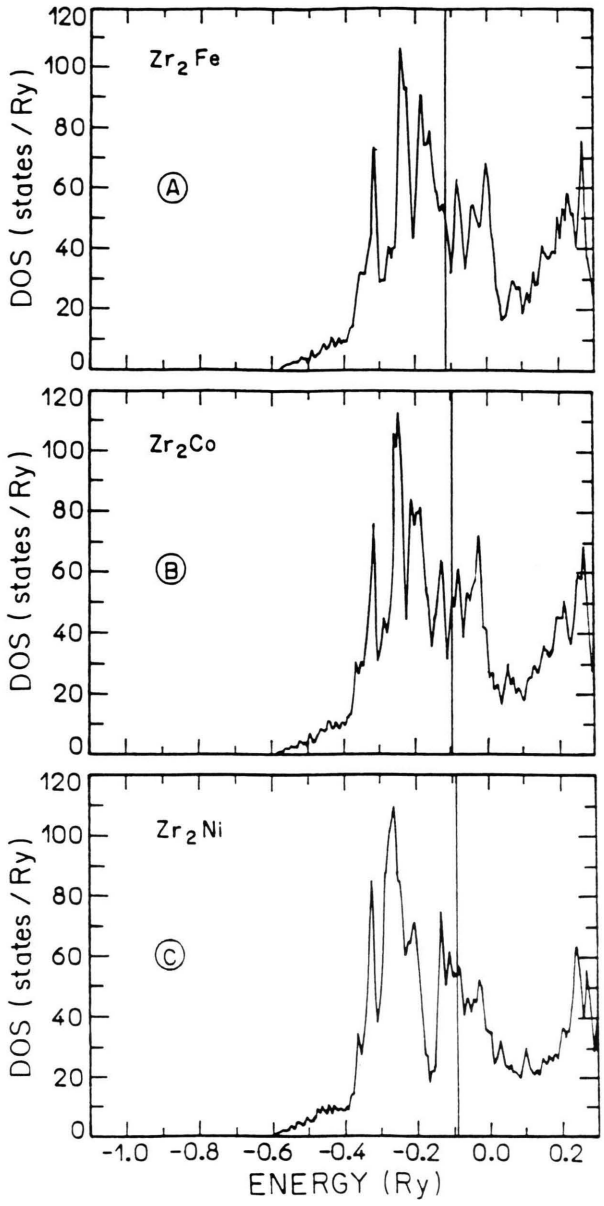

Fig. 3. Total density of states for a) Zr_2Fe, b) Zr_2Co and c) Zr_2Ni.

consequence, the charge transfers are small (see Table 1), which is a general feature of transition metal alloys [4, 14]. The $N(E_f)$ rises continuously from Zr_2Fe to Zr_2Ni. This interesting feature results from two different contributions that can be seen in Figure 2. The LDOS at both the Zr and T site is always dominated by the *d* partial contribution, but the T site has a much higher peak (well below E_f) that becomes higher and goes to lower energies as we go from Fe to Ni, adding one more electron. The general shape of the Zr LDOS is more or less the same in the three compounds, keeping essentially the same width, but showing different structures after the first energy peak, that is located where the *s* projected LDOS has a peak. The LDOS at the Fermi level at the T site decreases from Fe to Ni, but the LDOS at the Zr site has the opposite behaviour, that is, it increases from Fe to Ni. Comparing both sites in a given compound,we see that, at E_f, the LDOS for the Zr site is much larger than that of the Ni site in Zr_2Ni, is slightly larger than that of the Co site in Zr_2Co, and is slightly smaller than the LDOS at the Fe site. The total DOS is made by two times the Zr LDOS plus the transition metal T LDOS (Zr_2T), so the total $N(E_f)$ is generally dominated by the Zr LDOS in all compounds studied here.

In Table 2 we show our calculated values for the total EFG tensor components $\bar{V}_{ij}$ and its *p* and *d* contributions at the Zr site. There is also a very small *s-d* contribution to the EFG tensor with a magnitude never larger than 2×10^{13} esu/cm^3, which is responsible for the different values attained by the sum of the *p* and *d* contributions and the total $\bar{V}_{ij}$ components in Table 2. At the Zr site in all Zr_2T compounds considered here, the symmetric EFG tensor is not diagonal, but the components $\bar{V}_{xz}$ and $\bar{V}_{yz}$ are zero and we only show the three non zero components in Table 2. For this site, the $\bar{V}_{xy}$ component was found to be positive and much larger than the diagonal components. As we can see, the *p* contribution is dominant for all EFG tensor components at the Zr sites, being much larger than the *d* contribution as a general rule, with the only exception of the $\bar{V}_{zz}$ at Zr_2Ni, where the *p* and *d*

Table 2. Total EFG tensor components and its *p* and *d* contributions (in units of 10^{13} esu · cm^{-3}) at the Zr site in the Zr_2T compounds.

		Total	*p*	*d*
$\bar{V}_{xy}$	Zr_2Fe	+376	+349	+24
	Zr_2Co	+319	+332	−15
	Zr_2Ni	+158	+215	−60
$\bar{V}_{zz}$	Zr_2Fe	−72	−68	−4
	Zr_2Co	−126	−100	−28
	Zr_2Ni	−4	+24	−28
$\bar{V}_{xx} = \bar{V}_{yy}$	Zr_2Fe	+36	+34	+2
	Zr_2Co	+63	+50	+14
	Zr_2Ni	+2	−12	+14

contributions are almost equal and have opposite signs. Taking the sign into account, we can see that the *p* and *d* contributions (and so does the total contribution) for $\bar{V}_{xy}$ at the Zr site, increase continuously from Zr_2Ni to Zr_2Co and Zr_2Fe. Looking now to the $\bar{V}_{zz}$ component at the Zr site in Table 2 we see that, although it is always negative in the three compounds, it is almost zero in Zr_2Ni, and much larger in Zr_2Co than in Zr_2Fe. The almost vanishing value at Zr_2Ni comes from a particular cancellation between the *p* and *d* contributions, that have almost the same magnitude but opposit signs. However, in Zr_2Co and Zr_2Fe both contributions have the same sign and add together to form the total $\bar{V}_{zz}$, but as both are smaller in Zr_2Fe (with an almost zero value for the *d* contribution), $\bar{V}_{zz}$ becomes much larger in Zr_2Co.

The values of the radial *p* and *d* integrals at the Zr and T sites are given in Table 3. We see that I_{pp}^{Zr} is an order of magnitude larger than I_{dd}^{Zr} (reflecting the $\bar{V}_{ij}$ trend observed in Table 2), and both have almost constant values: I_{pp}^{Zr} varies by not more than two percent from one compound to the other, and I_{dd}^{Zr} does not vary. The change of I_{pp}^{Zr} can be explained by the small decrease of the WS radius (see Table 1), a more compressed *p* wave function adding more weight at the region near the nucleus; the I_{dd}^{Zr} are not sensible to such changes, as discussed in [3, 4, 7, 8, 13]. Looking now at the T site radial integrals from Table 3, we see that the I_{dd}^{T} are much larger than at the Zr site, increasing continuously with the *d* band filling from Fe to Ni, while I_{pp}^{T} remains almost constant and much smaller than at the Zr sites. These effects reflect the very different electronic structure of the early and late transition metals.

In Table 4 we compare the trends of theoretical and experimental results for the EFG and η at the Zr site. The theoretical values have been obtained from the diagonalization of the EFG tensor ($\bar{V}_{ij}$) shown in Table 2. In Table 4 we also show the eigenvalues (V_{ii} components of the tensor after diagonalization) and corresponding eigenvectors (direction cosines of the principal axes with respect to the *a*, *b*, and *c* axes of the structure) for the total components at the Zr sites. In all compounds the three eigenvectors are the same, and the *c* axis is one of the principal axes of the tensor, but for the other axes we have a rotation of 45° in the *x*-*y* plane. The direction of the EFG is in the plane perpendicular to the *c* axis and makes a 45° angle with the *a* and *b* axes. A comparison of the theoretical and experimental values shown in Table 4 cannot be made directly, because in the TDPAC experiment [9, 10] a ^{181}Ta probe was used at the place of Zr. We also note that the TDPAC technique cannot determine the EFG sign, so the measured values shown in Table 4 are absolute values. Despite that fact, the trends of that the measured and theoretical EFGs are the same: the EFG increases strongly from Zr_2Ni to Zr_2Co and much less from Zr_2Co to Zr_2Fe. We note that the probe effect on the EFG results is strong since Ta and Zr have different electronic structure. An attempt to compare the theoretical and experimental results can be made as suggested in [7]. The EFG at ^{181}Ta in hcp Zr has been measured by the TDPAC to be 514×10^{15} V/cm^2 [15], the EFG at Zr in Zr has been measured by NMR to be 368×10^{15} V/cm^2 [15]. The ratio between those two values is around 1.4. By multiplying the theoretical Zr EFG values in Table 4 by this factor we find a very reasonable overall agreement between the theoretical and measured EFG results.

Table 3. Radial *p* and *d* integrals (in Å^{-3}) for the Zr and T site in the Zr_2T compounds.

Zr_2T	Zr_2Fe	Zr_2Co	Zr_2Ni
I_{pp}^{Zr}	121.9	124.4	126.2
I_{dd}^{Zr}	11.5	11.5	11.6
I_{pp}^{T}	68.2	70.4	69.6
I_{dd}^{T}	30.0	36.8	44.4

Table 4. Theoretical EFGs (in 10^{13} esu · cm^{-3}) and asymmetry parameters η (dimensionless) for the Zr site in the Zr_2T compounds as compared with EFG (exp) and η (exp), from [9] and [10]. Theoretical eigenvalues (EFG tensor components in the principal axes) and corresponding eigenvectors of this rotation are also shown.

Zr_2T (Zr site)	EFG	EFG (exp)	η	$\eta_{(exp)}$	Eigenvalues	Eigenvectors
Zr_2Fe	+412	±607 (3)	0.65	0.82 (1)	+412	(−0.707; −0.707; 0.0)
					−340	(−0.707; +0.707; 0.0)
					−72	(0.0; 0.0; 1.0)
Zr_2Co	+382	±520 (3)	0.34	1.00 (1)	+382	(−0.707; −0.707; 0.0)
					−256	(−0.707; +0.707; 0.0)
					−126	(0.0; 0.0; 1.0)
Zr_2Ni	+160	±367 (2)	0.94	0.83 (1)	+160	(−0.707; −0.707; 0.0)
					−156	(−0.707; +0.707; 0.0)
					−4	(0.0; 0.0; 1.0)

An other comparison we have made in the following way: We have performed self consistent calculations for bulk Ta in a hypothetical hcp structure with the Zr lattice parameters, and for bulk Zr in the same hcp structure, both with the WS radius 1.771 Å. We have obtained 255 and 117 $Å^{-3}$ for Ipp in Ta and Zr, respectively, which gives a ratio $[I_{pp}(\mathrm{Ta})/I_{pp}(\mathrm{Zr})] \cong 2.2$, a factor that is not far from the 1.4 factor mentioned above. We note that the EFG is a very sensible quantity that depends on very small differences (of the order of 0.01 electrons) between occupations of orbitals with different symmetry around the nucleus. Taking this into account, we see that the agreement reached in the present study (where the ASA approximation is used) is reasonable, considering the lack of adjustable parameters and the subtlety of the effect.

Coming to Table 4, we see that the calculated η at the Zr site in Zr_2Ni and Zr_2Fe is large, in agreement with the measurements, while the small value in Zr_2Co does not agree with measurement. That η is almost one at Zr_2Ni comes from the fact that one EFG diagonal tensor component (eigenvalues shown at Table 4) is almost zero, which makes the other two components almost equal and with opposite signs (we must note that in this situation the EFG can easily change its sign). As noted by Havinga et al. [11] and mentioned above, in the Zr_2Ni crystal the x and c/a parameters make the hexagons of the structure very regular, so this extremely large η value in Zr_2Ni may be due to a special situation regarding symmetry. The relatively small η value in Zr_2Co comes from the fact that the original $\bar{V}_{zz}$ (component along the c axis) is much larger in Zr_2Co than in Zr_2Fe and Zr_2Ni. Also the cancellation between the p and d contributions to $\bar{V}_{zz}$ in Zr_2Ni, that does not happen in the other cases, leads to the very large η in Zr_2Ni.

Our theoretical results for the EFG at the T site in the Zr_2T compounds are shown in Table 5. The Fe, Co and Ni sites have axial symmetry along the axes parallel to the c crystal axes, so the EFG tensors are diagonal, with $\eta = 0$, at those sites. The EFG (V_{zz}, in Table 5) is along the c axes, negative at the Fe site but positive at the Co and Ni sites. For Fe we found good agreement with Mössbauer measurements, and the p and d contributions are negative and similar in magnitude (with a slightly larger d contribution). The Ni and Co V_{zz} have positive p and d contributions, both smaller than at the Fe site, and the d contribution at Ni is practically zero. Comparing the EFG values for Fe, Co and Ni sites, we cannot observe any remarkable trend. We only note that the general decrease of the p contribution of the late transition metals, compared to the Zr site, is probably related to the fact that its I_{pp} radial integrals are much smaller, as mentioned above and shown in Table 3.

Table 5. Contributions p (V_{zz}^{P}), d (V_{zz}^{d}) and the *total* (V_{zz}^{T}) EFG (in units of 10^{13} esu · cm^{-3}) at the T site in the Zr_2T compounds. The experimental value $V_{zz}^{(\mathrm{exp})}$ for ^{57}Fe in Zr_2Fe was obtained from a) [16] and b) [17].

Zr_2T (T site)	Zr_2Ni	Zr_2Co	Zr_2Fe
V_{zz}^{P}	+25	+21	−36
V_{zz}^{d}	+1	+8	−60
V_{zz}^{T}	+24	+28	−97
$V_{zz}^{(\mathrm{exp})}$	–	–	−110 (a) −134 (b)

3. Conclusions

We have performed k-space LMTO-ASA calculations to find the EFG trends at all sites in three different crystalline alloys with the same C16 type structure: Zr_2Fe, Zr_2Co and Zr_2Ni. The EFGs at Zr sites were compared with TDPAC measurements which use a ^{181}Ta probe. In all cases the calculated values reproduce the observed experimental trends of the EFG where the absolute value increases when going through the 3d metal series from Zr_2Ni to Zr_2Fe. We found a positive EFG at all Zr sites and also at Ni and Co sites, but a negative EFG at the Fe site in Zr_2Fe. We predict that the direction of the EFG is (110) for the Zr sites in all investigated compounds. Our theoretical η values are in reasonable agreement with the experimental values for the Zr site in Zr_2Fe and Zr_2Ni, where a large value, close to one, has been observed. The calculated η value for Zr in Zr_2Co is much smaller than the experimental one, and there may be a special influence of the probe in this case. Finally, we have seen that there is no particular correlation between the density of states at the Fermi level and the EFG value as it has been recently suggested for HfV_2H_x compounds [18]. We note that the EFG originates from small differences in occupations of orbitals of different symmetry around the nucleus, and these differences usually develop along the whole occupied bands. The fact that the partial LDOS have different shapes for different orbitals should be more important for the value of the EFG than the detailed behavior of the DOS at the Fermi level.

Acknowledgements

We wish to thank Dr. M. S. Methfessel and Professor O. K. Andersen and his group for making available to us the programs used in this work. We also wish to thank Dra. S. Frota-Pessôa for very useful discussions and careful reading of the manuscript. This work was partially supported by Fundação de Amparo à Pesquisa do Estado de São Paulo (FAPESP), Conselho Nacional de Desenvolvimento Científico e Tecnológico (CNPq) and Financiadora de Estudos e Projetos (FINEP).

[1] O. K. Andersen, Phys. Rev. B **12,** 3060 (1975).
[2] H. M. Petrilli, S. Frota-Pessôa, and M. Methfessel, Hyp. Int. **60,** 647 (1990).
[3] P. Blaha, K. Schwarz, and P. H. Dederichs, Phys. Rev. B **37,** 2792 (1988).
[4] H. M. Petrilli and S. Frota-Pessôa, Phys. Rev. B **44,** 10493 (1991) and references therein.
[5] S. Fereira and S. Frota-Pessôa, Phys. Rev. B **51,** 2045 (1995) and references therein.
[6] R. Coehoorn, R. H. J. Buschow, M. W. Dirken, and R. C. Thiel, Phys. Rev. B **42,** 4645 (1990).
[7] L. A. de Mello, H. M. Petrilli, and S. Frota-Pessôa, J. Phys. Condens Matter **5,** 8935 (1993).
[8] M. Methfessel and S. Frota-Pessôa, J. Phys. Condens. Matter **2,** 149 (1990).
[9] M. Marszalek, H. Saitovitch, P. R. J. da Silva, and A. Z. Hrynkiewicz, J. Alloys Compounds **219,** 128 (1995).
[10] B. Wodniecka, M. Marszalek, P. Wodniecki, and A. Z. Hrynkiewicz, Hyp. Int. **80,** 1039 (1993).
[11] E. E. Havinga, H. Damsma, and P. Hokkeling, J. Less-Common Met. **27,** 169 (1972).
[12] O. K. Andersen, O. Jepsen, and D. Glötzel, in Highlights of Condensed Matter Theory, edited by F. Bassani, F. Fumi, and M. P. Tosi, North-Holland, Amsterdam, 1985.
[13] H. M. Petrilli and S. Frota-Pessôa, J. Phys. Condens. Matter **2,** 135 (1990).
[14] S. Frota-Pessôa, Phys. Rev. B **28,** 3753 (1983).
[15] W. Witthuhn and W. Engel, in Hyperfine Interactions of Radioactive Nuclei, "Topics in Current Physics", vol. **31,** p. 205, ed. by J. Christiansen, Springer-Verlag, Berlin 1983, and references therein.
[16] F. Aubertin, U. Gonser, S. J. Campbell, and H. G. Wagner, Z. Metallk. **76,** 237 (1985).
[17] M. Maurer, J. M. Friedt, and J. P. Sanchez, J. Phys. F **15,** 1449 (1985).
[18] M. Forker, W. Herz, D. Simon, and S. C. Bedi, Phys. Rev. B **51,** 15994 (1995).